Comparative study of the anchoring strength of reactive mesogens and industrial polyimides used for the alignment of liquid crystals

T. Sergan,[1] I. Dozov,[2] V. Sergan,[1] and R. Voss[1]
[1]*California State University, Sacramento, 6000 J Street, Sacramento, California 95819, USA*
[2]*Université de Picardie Jules Verne, 80039 Amiens, France*
(Received 15 January 2017; published 31 May 2017)

We measured the Rapini-Papoular polar anchoring strength coefficient W for 4′-pentyl-4-cyanobiphenyl (5CB) on alignment layers formed by the reactive mesogen photopolymers RM 257, RM 82, and RM 84 [4,4′-bis(acryloyl)biphenyl] (by Merck). These materials are commonly used for the photostabilization of the liquid crystal (LC) director in the bulk as well as at the surface of the LC layer via the formation of a loose polymer network that captures the director orientation. We developed a method of fabrication of alignment layers from these polymers, and estimated W from the measurements of the optical retardation as a function of applied voltage in uniformly aligned cells. We found that RM 257 yielded W of about 6×10^{-4} J/m^2, whereas RM 82 and RM 84 provided anchoring strengths of about 2×10^{-4} and 4×10^{-4} J/m^2, respectively. Subsequent heating of the sample either destroyed the alignment layer, or substantially decreased W to about 1×10^{-4} J/m^2, which was comparable to the anchoring strength of weakly rubbed commercial polyimides.

DOI: 10.1103/PhysRevE.95.052706

I. INTRODUCTION

Liquid crystals (LCs) are usually studied in cells whose substrates provide well-defined boundary conditions that define the alignment of the LC molecules. The resultant orientation is determined by the anchoring properties of the alignment layer. The surface is usually given a treatment so that it imposes some preferred direction (easy axis) that determines the azimuthal orientation of the LC molecules. The alignment layer also anchors LC molecules at a certain polar (pretilt) angle which is determined by the surface-LC interactions. The surface alignment and anchoring energy strength are also of major importance for the technological applications of liquid crystals: The most important and widespread LC display technologies require well-defined in-plane and out-of-plane orientation of the nematic director on the boundary surfaces, and a predictable variation of this orientation under field during the device operation.

We are interested in the pretilt angle θ_{pretilt} and the anchoring strength coefficient W for a nematic liquid crystal on alignment layers formed by several reactive mesogen (RM)-type photopolymers, which are commonly used for the photostabilization of the liquid crystal director in the bulk and at the surface of the LC layer. These polymers have been extensively used for manufacturing polymer dispersed liquid crystals and liquid crystalline switchable optical elements, and the stabilization of various cholesteric and nematic devices via a polymer network created by the photopolymerization of reactive mesogens. It is well established that if this polymer network is formed in the liquid crystal phase of the material, it captures the image of the director field at the time of polymerization. The network retains order even at temperatures deep into the isotropic phase of the LC component, and induces a paranematic order in the LC matrix because of the anchoring of the LC molecules on the polymer bundles [1–5]. Indeed, due to the high surface-to-volume ratio of this LC-polymer composite, the surface anchoring energy plays an important role for both the stabilization of the nematic textures and the paranematic order induced in the isotropic phase.

Recently, we utilized low concentrations of RM-type photopolymers for the stabilization of molecular alignment in the vicinity of the LC layer boundary and developed a method of control of the pretilt angle in a continuous range of $2^\circ - 90^\circ$ [6–9]. We experimentally observed that certain photopolymers have a tendency to aggregate near the LC boundary, whereas others form a network within the bulk of the LC layer. Cells with an ordered polymer network in the bulk demonstrate strong residual birefringence effects in the isotropic phase, due to the induced nematiclike order at the interface between the photoaligned polymer and the isotropic phase of the mesogen. The studies of these paranematic effects are scarce; however, our research has shown that the effects are not only measurable but also quite significant, which has drawn our interest to the surface anchoring provided by photopolymers.

In this paper, we investigate the anchoring strength and the pretilt of the classical nematic material 4′-pentyl-4-cyanobyphenyl (5CB) on alignment layers formed by several RM-type photopolymers, namely, RM 257, RM 82, and RM 84 (BAB). We develop a method of fabrication of the alignment layer from the RM-type photopolymers and we measure the pretilt angle and the anchoring strength coefficient W of 5CB on these layers by using an electro-optic technique. We compare the results with the corresponding parameters for commercially deposited polyimide (PI 2555, Dupont), which was either hand or machine rubbed.

II. ANCHORING STRENGTH COEFFICIENT FROM THE OPTICAL RETARDATION VERSUS VOLTAGE MEASUREMENTS

In our work we employ a method of measurement of the anchoring strength coefficient from the measurement of the optical retardation R of a uniformly aligned LC cell as a function of applied voltage V (described in Refs. [10–13]) that requires minimization of the free energy of the

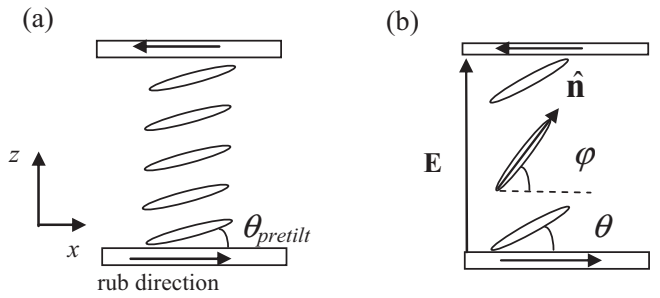

FIG. 1. Director configuration (a) without and (b) with an applied electric field.

cell F,

$$F = \int_0^d f_{\text{bulk}} dz + 2f_s(\theta) = \frac{1}{2}\int_0^d [k_{11}(\nabla\cdot\hat{\mathbf{n}})^2 + k_{33}[\hat{\mathbf{n}}\times[\nabla\times\hat{\mathbf{n}}]]^2 + \mathbf{D}\cdot\mathbf{E}]dz + 2f_s(\theta), \quad (1)$$

where the z axis is perpendicular to the cell substrates, $\hat{\mathbf{n}}$ is the LC director, d is the cell gap, k_{11} and k_{33} are the splay and bend elastic constants, respectively, $\mathbf{D}$ is the electric displacement, and $\mathbf{E}$ is the electric field with $\mathbf{D} = \varepsilon_0\boldsymbol{\varepsilon}\cdot\mathbf{E}$, where $\boldsymbol{\varepsilon}$ is the dielectric permittivity tensor, and the function $f_s(\theta)$ is the surface anchoring energy per unit area. Let us select a system of coordinates as shown in Fig. 1 and recast Eq. (1) by using the angle φ,

$$F = \frac{1}{2}\int_0^d \left[(k_{11}\cos^2\varphi + k_{33}\sin^2\varphi)\left(\frac{d\varphi}{dz}\right)^2 + \frac{D_z^2}{\varepsilon_0(\varepsilon_\parallel\sin^2\varphi + \varepsilon_\perp\cos^2\varphi)}\right]dz + 2f_s(\theta), \quad (2)$$

where $\varepsilon_\parallel$ and $\varepsilon_\perp$ are the dielectric permittivities parallel and perpendicular to the director, respectively.

The surface energy has no well-defined form, and is still a subject of extensive research [14]. The aligning surface orients the director along the easy axis. For small angles the energy per unit surface can be presented in the Rapini-Papoular form,

$$f_s(\theta) = \tfrac{1}{2}W\sin^2(\theta - \theta_{\text{pretilt}}), \quad (3)$$

where θ_{pretilt} is the director angle at the boundary of the nematic layer in the absence of applied voltage and $\theta = \varphi(0) = \varphi(d)$ when voltage is applied. The energy cost of the angular deviation of the director from the easy axis is characterized by an anchoring coefficient W which depends on the nature of the surface-LC interactions. W can be determined from the optical retardation curves as a function of applied voltage across the uniformly aligned cell with antiparallel rub directions [10,11]. We obtain the Euler-Lagrange equation according to the variational calculus,

$$(k_{11}\cos^2\varphi + k_{33}\sin^2\varphi)\varphi'' + (k_{33} - k_{11})(\sin\varphi\cos\varphi)(\varphi')^2 + \frac{D_z^2(\varepsilon_\parallel - \varepsilon_\perp)\sin\varphi\cos\varphi}{\varepsilon_o(\varepsilon_\perp\cos^2\varphi + \varepsilon_\parallel\sin^2\varphi)^2} = 0, \quad (4)$$

where the prime denominates differentiation with respect to z. After multiplication by $2\varphi'$, Eq. (4) can be presented in the following form,

$$\frac{d}{dz}\left((k_{11}\cos^2\varphi + k_{33}\sin^2\varphi)(\varphi')^2 - \frac{D_z^2}{\varepsilon_o(\varepsilon_\parallel\sin^2\varphi + \varepsilon_\perp\cos^2\varphi)}\right) = 0, \quad (5)$$

and then integrated. The integration constant can be determined from symmetry of the solution about the cell's midpoint as the angle φ reaches a maximum in the middle of the cell,

$$\left(\frac{d\varphi}{dz}\right)^2 = \frac{\gamma D_z^2}{k_{11}\varepsilon_o\varepsilon_\perp}\frac{\sin^2\varphi_{\max} - \sin^2\varphi}{(1+\kappa\sin^2\varphi)(1+\gamma\sin^2\varphi)(1+\gamma\sin^2\varphi_{\max})}, \quad (6)$$

where $\varphi|_{z=d/2} = \varphi_{\max}$, $\gamma = (\varepsilon_\parallel - \varepsilon_\perp)/\varepsilon_\perp = \Delta\varepsilon/\varepsilon_\perp$, $\kappa = (k_{33} - k_{11})/k_{11}$, and

$$D_z = \frac{\varepsilon_o V}{\int_0^d \left(\frac{1}{\varepsilon_\perp\cos^2\varphi + \varepsilon_\parallel\sin^2\varphi}\right)dz} = \text{const}, \quad (7)$$

where V is the applied voltage.

The balance of torques on the surface $\pm\frac{\partial f_{\text{bulk}}}{\partial\varphi'}|_{z=0} + \frac{\partial f_s}{\partial\theta} = 0$ gives the following boundary condition for Eqs. (4) and (5) [10–11,14]:

$$(k_{11}\cos^2\theta + k_{33}\sin^2\theta)\left.\frac{\partial\varphi}{\partial z}\right|_{z=0} = \frac{1}{2}W\sin[2(\theta - \theta_{\text{pretilt}})]. \quad (8)$$

Integrating Eq. (6) from $z = d/2$ to $z = 0$, one can express D_z as

$$D_z = \frac{1}{d}\sqrt{\frac{k_{11}\varepsilon_o\varepsilon_\perp}{\gamma}}\sqrt{1+\gamma\zeta_m}\int_{\zeta_b}^{\zeta_m}\sqrt{\frac{(1+\gamma\zeta)(1+\kappa\zeta)}{(\zeta_m - \zeta)\zeta(1-\zeta)}}d\zeta, \quad (9)$$

where $\zeta = \sin^2\varphi$, $\zeta_m = \sin^2\varphi_{\max}$, and $\zeta_b = \sin^2\theta$. W can be expressed using D_z in the following form,

$$W = \frac{2k_{11}}{d\sin[2(\theta - \theta_{\text{pretilt}})]}\frac{\sqrt{(1+\kappa\zeta_b)(\zeta_m - \zeta_b)}}{\sqrt{1+\gamma\zeta_b}}I_D(\zeta_b,\zeta_m), \quad (10)$$

where

$$I_D(\zeta_b,\zeta_m) = \int_{\zeta_b}^{\zeta_m}\sqrt{\frac{(1+\gamma\zeta)(1+\kappa\zeta)}{(\zeta_m - \zeta)\zeta(1-\zeta)}}d\zeta. \quad (11)$$

The optical retardation of the cell is given by

$$R = \frac{4\pi}{\lambda}\int_0^{d/2}\left(\frac{n_o n_e}{\sqrt{n_e^2\sin^2\varphi + n_o^2\cos^2\varphi}} - n_o\right)dz, \quad (12)$$

where n_o and n_e are the refractive indices for the ordinary and extraordinary waves, respectively, and λ is the wavelength of light.

Using $d\varphi/dz$ from Eq. (6) and integrating over the cell thickness, one can express D_z through I_D, and then calculate R,

$$R = \frac{2\pi d n_o \nu}{\lambda I_D(\zeta_b,\zeta_m)} I_R(\zeta_b,\zeta_m), \tag{13}$$

where

$$I_R(\zeta_b,\zeta_m) = \int_{\zeta_b}^{\zeta_m} \sqrt{\frac{(1-\zeta)(1+\gamma\zeta)(1+\kappa\zeta)}{\zeta(\zeta_m-\zeta)[1-\nu(1-\zeta)]}} \frac{d\zeta}{1+\sqrt{1-\nu(1-\zeta)}} \tag{14}$$

and $\nu = \frac{n_e^2-n_o^2}{n_e^2}$.

The applied voltage is given by

$$V = \int_0^d E_z dz = \frac{2D_z}{\varepsilon_o}\int_0^{d/2} \frac{dz}{\varepsilon_\perp \cos^2\varphi + \varepsilon_\parallel \sin^2\varphi} = \frac{V_{\rm th}}{\pi}\sqrt{1+\gamma\zeta_m} I_V(\zeta_b,\zeta_m), \tag{15}$$

where

$$I_V(\zeta_b,\zeta_m) = \int_{\zeta_b}^{\zeta_m} \sqrt{\frac{1+\kappa\zeta}{(\zeta_m-\zeta)\zeta(1-\zeta)(1+\gamma\zeta)}} d\zeta, \tag{16}$$

and

$$V_{\rm th} = \pi\sqrt{\frac{k_{11}}{\varepsilon_o \Delta\varepsilon}} \tag{17}$$

is the Fréedericksz's transition threshold.

The anchoring coefficient W can be determined using the above equations, however, a simplified R vs V relationship is more desired for practical applications. An approximation was proposed by Nastishin *et al.* [10,11], based on the asymptotic behavior of the integrals I_D, I_V, and I_R when $\zeta_b \to \zeta_{\rm pretilt}$ with $\zeta_{\rm pretilt} = \sin^2\theta_{\rm pretilt}$ and $\zeta_m \to 1$. The integrals can be expanded in terms of $\sin(\theta - \theta_{\rm pretilt})$ and only the linear terms are kept. This leads to a limited voltage range within which the technique can be applicable. The details of the procedure are described in Ref. [11], where the authors limited the angle deviations to $|\theta - \theta_{\rm pretilt}| < 0.2$ rad; this gave an upper voltage limit $V_{\rm max} = \frac{0.2}{\pi\cos\theta_{\rm pretilt}}\sqrt{\frac{\varepsilon_\perp}{\varepsilon_\parallel}}\frac{Wd}{k_{11}} V_{\rm th}$, whereas the condition of $1-\zeta_m < 3\times10^{-6}$ set the lower voltage limit $V_{\rm min} = 6V_{\rm th}$. In this approximation R vs V is given as follows,

$$\frac{R(V-V^*)}{R_0} = Y - \frac{2k_{11}}{Wd}(1+\kappa\sin^2\theta_{\rm pretilt})(V-V^*), \tag{18}$$

where

$$R_0 = \frac{2\pi d n_o \nu \cos^2\theta_{\rm pretilt}}{\lambda(1+\sqrt{1-\nu\cos^2\theta_{\rm pretilt}})\sqrt{1-\nu\cos^2\theta_{\rm pretilt}}} \tag{19}$$

is the retardation in the absence of electric field,

$$V^* = \frac{1}{\pi}\frac{\Delta\varepsilon}{\varepsilon_\parallel} V_{\rm th}\int_{\zeta_{\rm pretilt}}^1 \sqrt{\frac{(1+\gamma)(1+\kappa\zeta)}{\zeta(1+\gamma\zeta)}} d\zeta, \tag{20}$$

and Y is a constant given by

$$Y = \frac{V_{\rm th}}{\pi}\left(1 - \frac{2k_{11}}{Wd}\frac{\gamma(1+\kappa\sin^2\theta_{\rm pretilt})\cos^2\theta_{\rm pretilt}}{1+\gamma\sin^2\theta_{\rm pretilt}}\right) \times \frac{(1+\sqrt{1-\nu\cos^2\theta_{\rm pretilt}})\sqrt{1-\nu\cos^2\theta_{\rm pretilt}}}{\cos^2\theta_{\rm pretilt}\sqrt{1+\gamma}} I_R(\zeta_{\rm pretilt},1), \tag{21}$$

where

$$I_R(\zeta_{\rm pretilt},1) = \int_{\zeta_{\rm pretilt}}^1 \sqrt{\frac{(1+\kappa\zeta)(1+\gamma\zeta)}{\zeta[1-\nu(1-\zeta)]}} \times \frac{d\zeta}{[1+\sqrt{1-\nu(1-\zeta)}]}.$$

The slope of Eq. (18) is proportional to the reciprocal of the anchoring strength W, which makes this method applicable for the weak and intermediate anchoring strengths and problematic for strong anchoring. In our work we have taken the experimental values of $V_{\rm th}$ and R_0 to calculate W rather than the ones calculated from Eqs. (17) and (19). Finally, Eq. (18) can be used to fit the linear portion of the actual $R(V-V^*)$ vs $(V-V^*)$ curve.

When fitting the experimental data, $V_{\rm min} = 6V_{\rm th}$ and $V_{\rm max}$ were determined from the requirement that the second term in Eq. (18) is 20% of the first term, as suggested in Ref. [11].

III. EXPERIMENT

A. Materials, fabrication of the alignment layer, and LC cells

To prepare an alignment layer, we dissolved RM 257 in a solvent (S33 by Nissan, commonly used to dissolve polyimides) at about 10% by weight; the photoinitiator was added to the mixture at a concentration of 0.005 wt %. The solution was spin coated at 4000 rpm on indium-tin oxide (ITO) coated glass substrates. Films made of RM 257 were polymerized for 1 h with UV light by using a black mineral lamp (100 μW/cm^2 in both the UVA and UVB range) while the materials are in an isotropic phase, at about 140 °C, and hand rubbed 20 times in one direction with a velvet cloth attached to a 1 lb. block applying a pressure of about 35 g/cm^2; this technique is employed to induce an easy axis and provide for strong anchoring in noncommercial settings.

RM 84 (BAB) and RM 82 were dissolved in N-methyl-2-pyrrolidone (5% by weight, photoinitiator added), and spin coated on ITO-covered glass substrates at 4000 rpm. The materials were photopolymerized at 160 °C for 1 h and hand rubbed in the same manner as RM 257.

All cells were assembled with antiparallel rub directions with 20-μm fiber spacers in the gasket. An examination of the empty planar cells under a polarizing microscope equipped with Berek compensator revealed that they possessed an in-plane optical retardation of less than 1 nm. The cells were filled with 5CB and examined again. We assumed the following dielectric and elastic constants for 5CB: $\varepsilon_\parallel = 17.5$ and $\varepsilon_\perp = 6.0$ [15], and $k_{11} = 6.65\times10^{-12}$ N, $k_{33} = 8.95\times10^{-12}$ N, $n_o = 1.530$, and $n_e = 1.717$ [10,11].

The pretilt angle was measured by using a crystal rotation method [16] for the cells both before and after heating (in cases

when cells were heated in order to eliminate nonuniformities and defects). The pretilt angle was about 1° in all cases; it changed only slightly after heating. We did not find any significant difference in the pretilt angle at different cell sites.

In order to compare the alignment properties of photopolymers with polyimides we prepared two planar cells with a PI 2555 (Dupont) alignment layer according to the manufacturer's instructions. Alignment was produced by rubbing each substrate with a velvet cloth (attached to a 1 lb. block) in one direction. We rubbed the PI either lightly (applying a pressure of 10 g/cm^2), or strongly (applying a pressure of 35 g/cm^2) which corresponded to two practical cases that occurred during preparation of the alignment layers for research purposes.

B. Optical measurement techniques

Optical retardation was measured by using the Senarmont method [11,17], a null ellipsometry technique that utilizes a fixed polarizer, a quarter-wave plate with an optical axis parallel to the polarizer, and a rotating analyzer. A cell is placed between the polarizer and quarter-wave plate with the rub direction at 45° to the transmission axis of the polarizer. Light exiting the polarizer has vertical and horizontal components of equal intensity with no phase shift between them. The LC cell introduces a phase shift, thus the light coming out of the sample is elliptically polarized. After passing through a quarter-wave plate, it becomes almost linearly polarized at some angle ψ with respect to the direction of the transmission axis of the polarizer. The angle ψ is measured by rotating the analyzer to the position of maximum light extinction. The absolute phase shift between the ordinary and extraordinary waves R is related to ψ as $R = 2\psi$. In our measurements we used a ratio of ψ/ψ_0 without direct calculations of the optical retardation at each applied voltage level, therefore, Eq. (18) can be rewritten in terms of the measured quantities as

$$\frac{\psi(V - V^*)}{\psi_0} = Y - \frac{2k_{11}}{Wd}(1 + \kappa \sin^2\theta_{\text{pretilt}})(V - V^*). \quad (22)$$

Hereafter we will use $\psi(V - V^*)/\psi_0$ vs $(V - V^*)$ dependencies to discuss all experimental data.

The initial optical retardation R_0 was calculated by adding all subsequent phase shifts (measured each time the applied voltage is increased by a small step) plus the residual birefringence (measured at the highest applied voltage). These precision measurements took into account the shrinking of the cell gasket after heating from room temperature to 25 °C, which caused a slight change in R_0.

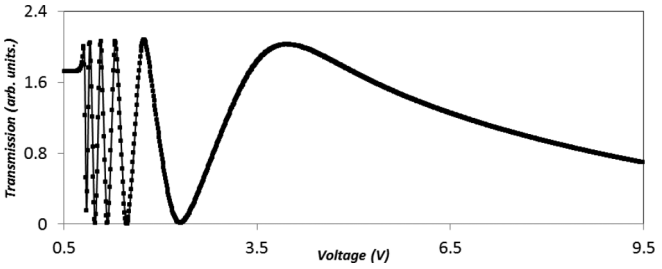

FIG. 2. *T-V* curve for 5CB on RM 82 cell No. 2.

In our measurements we used testing light from an intensity-stabilized He-Ne laser ($\lambda = 633$ nm), and a quarter-wave plate (for all cells with the exception of RM 257 cell No. 1 before heating, for which we used a Babinet-Soleil compensator). ac voltage with a frequency $f = 1$ kHz was applied to the nonheated RM 257 cell No. 1 whereas all other cells were driven at $f = 5$ kHz. We used a data acquisition (DAQ) card and an external amplifier to apply voltage with a chosen frequency, square-wave shape, and amplitude (independently measured using an oscilloscope). The intensity of light transmitted through the ellipsometer was measured with a photodiode. The retardation measurements were performed at 25 °C by stabilizing the cell's temperature with the help of an MK-1 heating stage by Instec.

Because R_0 is high, it is difficult to measure it directly with acceptable precision. Thus it was measured using the following two methods. In the first method, an estimate of R_0 was made from the transmission versus voltage (T-V) curve measured when the cell was placed between crossed polarizers with its rub directions at 45° to the polarizer transmission axis. The T-V curve has an oscillatory character (see Fig. 2): The difference between the adjacent minimum and maximum on the curve corresponds to the change of retardation of π. This method was used as a checkpoint; it also provided data on Fréedericksz's threshold V_{th}.

To obtain an accurate value of R_0 we used the retardation versus voltage (R-V) measurement using the Senarmont technique described previously, and compared it to the one obtained from the T-V curves. We also measured the residual retardation of the cell at a temperature slightly above the nematic-to-isotropic state transition and

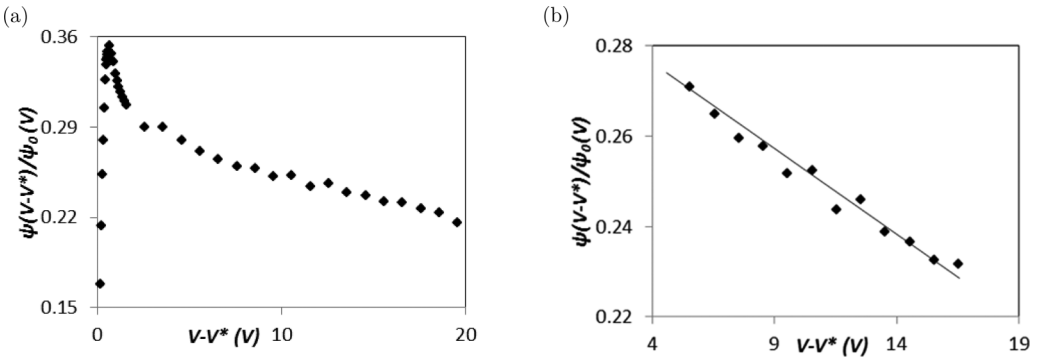

FIG. 3. $\psi(V - V^*)/\psi_0$ vs $(V - V^*)$ curve for 5CB on RM 82, cell No. 2.

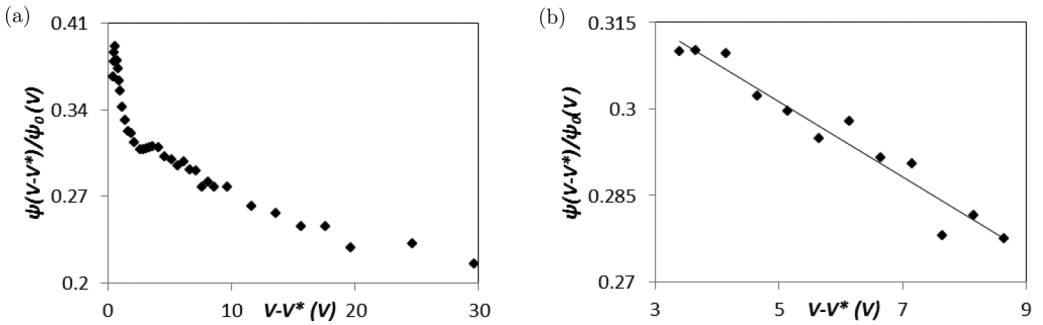

FIG. 4. $\psi(V - V^*)/\psi_0$ vs $(V - V^*)$ curve for 5CB on weakly rubbed PI 2555.

subtracted it from the cell's retardation before performing curve fitting.

We examined the in-plane nonuniformities due to rub irregularities leading to light scattering and azimuthal anchoring by introducing additional in-plane retardation of the cell. The latter was difficult to measure due to the arbitrary deviation of the grooves from the easy axis leading to a zero average of additional in-plane retardation. However, this effect contributed to light leakage when the cell's retardation was measured by a null ellipsometry technique. We found that heating the cells with RM 257 to 150 °C for 1 h eliminates most of the in-plane alignment irregularities, and decreases the light scattering and light leakage at the null position of the ellipsometer. Heating destroyed the alignment in cells with RM 82 and RM 84 (BAB) alignment layers, however, the untreated cells with these polymers did not demonstrate significant light scattering, and hence did not require annealing.

The technique of W measurement described in Refs. [10,11] requires estimation of the range of its applicability. The minimum voltage $V_{\min}$ is given by $6V_{\text{th}}$, where V_{th} is obtained from T-V curves. The upper limit $V_{\max}$ is determined from the condition that the second term in Eq. (18) does not exceed 20% of the value of constant Y. Because $V_{\max}$ depends on the anchoring coefficient W, we applied the following procedure: First, we identified a linear portion of the curve with a negative slope at $V > V_{\min}$, then we estimated W for the voltage interval above $V_{\min}$, and calculated $V_{\max}$. After that, we recalculated W for the found $V_{\max}$. The process was repeated until we converged on some W and $V_{\max}$, which were then accepted as true values for a given material.

C. Pretilts and anchoring strength coefficients for 5CB on RM and PI 2555 polymers

As an example of the analyzed curves we present data for planar cell No. 2 with RM 82 as an alignment layer. The thickness of this cell was measured at 20.0 μm when empty. It had $\theta_{\text{pretilt}} = 0.8°$. We applied ac voltage with a frequency of 5 kHz to drive this cell between 0 and 30 V. The Fréedericksz's threshold voltage estimated from the T-V curve was $V_{\text{th}} = 0.71$ V (see Fig. 2). Total head-on optical retardation (estimated from the residual retardation at high voltage) was $R_0 = 2\psi_0 = 33.6$ rad for red light ($\lambda = 633$ nm) which, according to Eq. (19), corresponded to $d = 18.1$ μm. The residual retardation at the temperature slightly above the nematic-to-isotropic state transition was about 0.1°. With the calculated value $V^* = 0.426$ V, the measured $\psi(V - V^*)/\psi_0$ vs $V - V^*$ curve (see Fig. 3) had a negative slope for the range of $(V - V^*) = 4 - 30$ V. The linear fit for the voltages in the range from $V_{\min} = 4.2$ V to $V_{\max} = 17.2$ V yielded the anchoring strength coefficient $W = (1.9 \pm 0.1) \times 10^{-4}$ J/m^2.

Figure 4 shows $\psi(V - V^*)/\psi_0$ vs $V - V^*$ curves for 5CB on weakly rubbed PI 2555, which we present here for comparison. Data on other studied alignment layers are summarized in Table I.

IV. DISCUSSION

The error bars for the anchoring coefficients W in Table I, which are calculated from the uncertainty of the slope of the $\psi(V - V^*)/\psi_0$ vs $V - V^*$ curves, vary rapidly with anchoring strength. For the weakest anchorings, e.g., $W < 1.5 \times 10^{-4}$ J/m^2 measured for the RM 257 (cell No. 1

TABLE I. Cell parameters, measured pretilt angles, and anchoring strength coefficients for 5CB on RM polymer alignment layers.

Alignment layer	θ_{pretilt}	V_{th} (V)	V^* (V)	Fitting range (V)	R_0 (rad)	d (μm) [from Eq. (19)]	W (J/m^2)
RM 257 cell No. 1 before heating	0.7°	0.81	0.465		34.7	18.6	No negative slope for $V > V_{\text{th}}$
RM 257 cell No. 1 after heating	0.7°	0.78	0.469	4.7–7.1	32.8	17.6	$(1.4 \pm 0.2) \times 10^{-4}$
RM 257 cell No. 2 before heating	1.5°	0.81	0.479	4.9–31.1	36.2	19.5	$(5.6 \pm 0.5) \times 10^{-4}$
RM 257 cell No. 2 after heating	1.1°	0.77	0.460	4.6–9.0	34.5	18.6	$(1.7 \pm 0.3) \times 10^{-4}$
RM 82 cell No. 1	0.8°	0.78	0.468	3.5–11.1	32.2	17.4	$(2.2 \pm 0.2) \times 10^{-4}$
RM 82 cell No. 2	0.8°	0.71	0.426	4.2–17.2	33.6	18.1	$(1.9 \pm 0.1) \times 10^{-4}$
RM 84 (BAB)	0.7°	0.77	0.465	3.5–19.1	34.7	18.7	$(3.8 \pm 0.6) \times 10^{-4}$
PI 2555 weakly rubbed	1.5°	0.60	0.355	3.6–9.0	32.6	17.5	$(1.2 \pm 0.1) \times 10^{-4}$
PI 2555 strongly rubbed	3°	0.55	0.387		35.	19.3	No negative slope for $V > V_{\text{th}}$

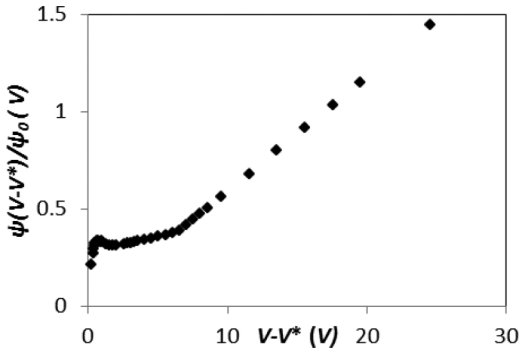

FIG. 5. $\psi(V - V^*)/\psi_0$ vs $(V - V^*)$ curve for 5CB on strongly rubbed PI 2555 (RM 257 cell No. 1 before heating demonstrates similar behavior).

after heating) and weakly rubbed PI 2555, the error is small, $\delta W \sim 2 \times 10^{-5}\,\mathrm{J/m^2}$. For stronger anchoring energies, the error increases, e.g., $\delta W \sim 6 \times 10^{-5}\,\mathrm{J/m^2}$ for RM 84 for which $W = 3.8 \times 10^{-4}\,\mathrm{J/m^2}$. Finally, for the highest anchoring energies, e.g., for strongly rubbed PI 2555, there is no negative-slope region in the $\psi(V - V^*)/\psi_0$ vs $V - V^*$ function (see Fig. 5) and the technique used in the present study is clearly not applicable.

This difficulty to measure strong anchoring energies is common for all the experimental techniques which are based on an extrapolation to high voltages of the retardation data measured at moderate voltages [10–12]. In fact, these techniques are not robust against a small additive error δR in the measured retardation $R(V)$. This spurious retardation may come from small imperfections in the optical setup and, more importantly, from the residual birefringence of the alignment layers and of the glass plates of the cell, which are distorted under mechanical stress. Although the influence of this spurious retardation is minimized in our experiment by subtracting the residual retardation measured in the isotropic state above the transition temperature T_c, it is practically impossible to get rid of it completely because of the δR variation with the temperature and with the applied voltage.

In Fig. 6 we present the numerical simulation of the influence of a small spurious retardation δR on the slope of the $R(V - V^*)/(V_{\mathrm{th}} R_0)$ vs $(V - V^*)/V_{\mathrm{th}}$ curve for two different anchoring strengths. For a very strong anchoring, $W = 1.3 \times 10^{-3}\,\mathrm{J/m^2}$ (expected for the strongly rubbed PI 2555 layer), even a small additive error in the measured retardation, $\delta R = 2\,\mathrm{nm}$, seriously modifies the curve [see Fig. 6(a)]. For $\delta R < 0$ the slope increases, resulting in an apparent W value which is approximately half the real anchoring energy. For $\delta R > 0$ the sign of the slope is changing, similar to the positive slope observed by us for the two strongest anchoring polymers, namely, the strongly rubbed PI 2555 layer and the RM 257 cell No. 1 before heating. For the weaker anchoring case shown on Fig. 6(b), the slope is less sensitive to spurious retardation, but the measured value of the anchoring coefficient W is still significantly influenced by δR: For the moderate $\delta R = 5\,\mathrm{nm}$ value, the measured anchoring energy is modified by a factor of 2.

In principle, there exist measurement techniques for the anchoring energy [18–20] that are quite insensitive to an additive retardation error. Instead, to an extrapolation of the R vs V curves measured at moderate voltages, these techniques are based on a direct measurement of the retardation at high voltages, comparable to the "anchoring breaking threshold,"

$$V_c = \frac{Wd}{\pi k_{11}\sqrt{1+\kappa}} V_{\mathrm{th}}. \tag{23}$$

At this threshold voltage the anchoring torque cannot balance more the electric-field torque transmitted to the surface and the anchoring is "broken" [21–23]: The surface director aligns exactly parallel to the field, with $\theta = \pi/2$, as in the absence of surface anchoring energy. For $V < V_c$ the slope of the retardation curve dR/dV is finite, defined as for $V \ll V_c$ by Eqs. (8)–(17). However, at $V = V_c$ the slope jumps down to zero, as $R = 0$ for $V \geqslant V_c$. This sudden change in the slope is easily detectable and rather insensitive to even very high errors in the measured retardation (as long as δR varies smoothly with V), thus allowing one to measure reliably the anchoring energy coefficient W. However, for the 20-μm-thick cells

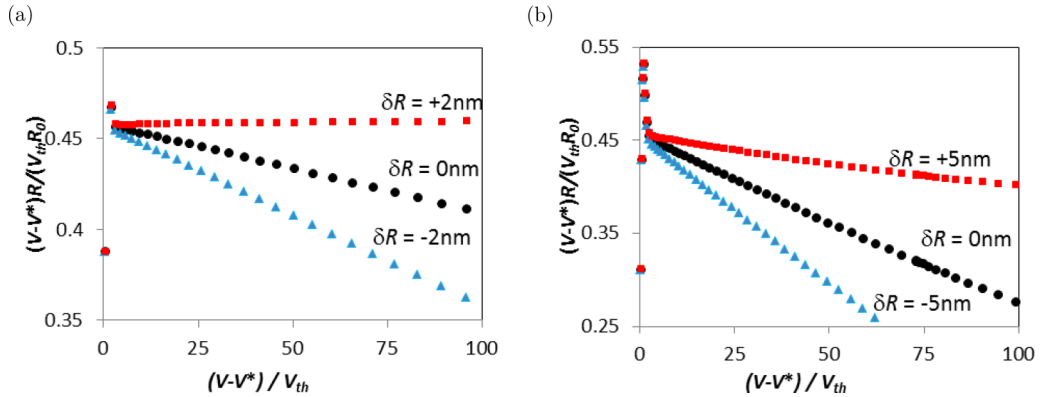

FIG. 6. Numerical simulation of the variation of the slope of the $R(V - V^*)/(V_{\mathrm{th}} R_0)$ vs $(V - V^*)/V_{\mathrm{th}}$ curves due to a small additive error δR in the experimentally measured retardation. (a) Very strong anchoring case, with $W = 1.3 \times 10^{-3}\,\mathrm{J/m^2}$ in the usual range for the surface energy on polyimide alignment layers; the slope of the curve is very sensitive to even small retardation errors and can even change its sign, making it impossible to measure the anchoring energy from the slope. (b) Moderately strong anchoring, with $W = 0.3 \times 10^{-3}\,\mathrm{J/m^2}$, similar to the anchoring energy coefficients measured on the photopolymer alignment layers. Although the slope is less sensitive to the retardation errors in this case, high δR values can still significantly influence the measured anchoring energies.

and $W = 3 \times 10^{-4}\,\mathrm{J/m^2}$ these methods require retardation measurements at voltages of about $300V_{\mathrm{th}}$. In our experiments, the cells were able to withstand up to $100V_{\mathrm{th}}$ applied, and thus high-voltage methods were not applicable. However, we intend to compare the high-voltage and intermediate-voltage methods in our future work.

V. CONCLUSIONS

We measured the polar anchoring strength coefficient W for 5CB on several types of alignment layers formed by photopolymers RM 257 (Merck), RM 82, and RM 84 (BAB). These polymers can be used in applications that require weak anchoring of LC. The present study also shows the significance of the effect of the anchoring of LC molecules by polymers that are commonly used for the stabilization of the liquid crystal director in the bulk and at the LC layer boundary, and helps to understand the anchoring of nematic molecules by polymer chains and observations of the paranematic state in the isotropic phase of a liquid crystal. We found that RM 257 yielded W of about $6 \times 10^{-4}\,\mathrm{J/m^2}$, whereas RM 82 and RM 84 provided anchoring strengths of about 2×10^{-4} and $4 \times 10^{-4}\,\mathrm{J/m^2}$, respectively. Heating either destroys the alignment layer formed from these polymers, or substantially decreases W to about $1 \times 10^{-4}\,\mathrm{J/m^2}$, which is comparable to the anchoring strength of weakly rubbed polyimides.

ACKNOWLEDGMENTS

We gratefully acknowledge discussions with S. Shiyanovskii. Our research was supported by Hu Foundation and NSM SURE program, CSUS.

[1] P. Sheng, Phys. Rev. A **26**, 1610 (1982).
[2] K. Miyano, Phys. Rev. Lett. **43**, 51 (1979).
[3] K. Miyano, J. Chem. Phys. **71**, 4108 (1979).
[4] G. P. Crawford, A. Scharkowski, Y. K. Fung, J. W. Doane, and S. Zumer, Phys. Rev. E **52**, R1273 (1995).
[5] *Liquid Crystals in Complex Geometries: Formed By Polymer and Porous Networks*, edited by G. P. Crawford and S. Zumer (Taylor and Francis, London, 1996).
[6] T. Sergan, V. Sergan, and P. Bos, Chem. Phys. Lett. **486**, 123 (2010).
[7] T. Sergan, V. Sergan, R. Herrera, L. Lu, P. J. Bos, and E. Sergan, Liq. Cryst. **40**, 72 (2013).
[8] L. Lu, T. Sergan, V. Sergan, and P. J. Bos, Appl. Phys. Lett. **101**, 251912 (2012).
[9] L. Lu, V. Sergan, and P. J. Bos, Phys. Rev. E **86**, 051706 (2012).
[10] Yu. Nastishin, R. D. Polak, S. Shiyanovskii, and O. Lavrentovich, Appl. Phys. Lett. **75**, 202 (1999).
[11] Yu. Nastishin, R. D.Polak, S. Shiyanovskii, V. H. Bodnar, and O. Lavrentovich, J.Appl. Phys. **86**, 4199 (1999).
[12] H. Yokoyama and H. A. van Sprang, J. Appl. Phys. **57**, 4520 (1985).
[13] S. Shiyanovskii (private communication).
[14] G. Barbero and L. R. Evangelista, *Absorption Phenomena and Anchoring Energy in Nematic Liquid Crystals* (Taylor and Francis, London, 2006).
[15] K. Abe, A. Usami, K. Ishida, Y. Fukushima, and T. Shigenari, J. Korean Phys. Soc. **46**, 220 (2005).
[16] K. Y. Han, T. Miyashita, and T. Uchida, Mol. Cryst. Liq. Cryst. **241**, 147 (1994).
[17] T. Sergan, V. Sergan, and B. MacNaughton, J. Display Technol. **3**, 29 (2007).
[18] M. Nobili and G. Durand, Phys. Rev. A **46**, R6174 (1992).
[19] I. Dozov, M. Nobili, and G. Durand, Appl. Phys. Lett. **70**, 1179 (1997).
[20] O. O. Ramdane, P. Auroy, S. Forget, E. Raspaud, P. Martinot-Lagarde, and I. Dozov, Phys. Rev. Lett. **84**, 3871 (2000).
[21] J. Nehring, A. R. Kmetz, and T. Scheffer, J. Appl. Phys. **47**, 850 (1976).
[22] G. Barbero and R. Barberi, J. Phys. (Paris) **47**, 609 (1983).
[23] I. Dozov and P. Martinot-Lagarde, Phys. Rev. E **58**, 7442 (1998).